**Atmospheric
Chemistry
and Physics**

Observations of high rates of NO_2-HONO conversion in the nocturnal atmospheric boundary layer in Kathmandu, Nepal

Y. Yu[1,*], **B. Galle**[1], **A. Panday**[2,**], **E. Hodson**[2,***], **R. Prinn**[2], and **S. Wang**[3]

[1]Optical Remote Sensing, Radio and Space Science, Chalmers University of Technology, 41296 Gothenburg, Sweden
[2]Dept. of Earth, Atmospheric, and Planetary Sciences, Massachusetts Institute of Technology, Cambridge, MA 02139, USA
[3]Jet Propulsion Laboratory, Pasadena, CA 91109, USA
[*]now at: Monitoring & Laboratory Division, California Air Resources Board, 9528 Telstar Avenue, El Monte, CA 91731, USA
[**]now at: Atmospheric and Oceanic Program, Princeton University, Princeton, NJ 08544, USA
[***]now at: Ecological Process Modelling Unit, Swiss Federal Institute for Forest, Snow and Landscape Research, Birmensdorf, 8903, Switzerland

Abstract. Nitrous acid (HONO) plays a significant role in the atmosphere, especially in the polluted troposphere. Its photolysis after sunrise is an important source of hydroxyl free radicals (OH). Measurements of nitrous acid and other pollutants were carried out in the Kathmandu urban atmosphere during January–February 2003, contributing to the sparse knowledge of nitrous acid in South Asia. The results showed average nocturnal levels of HONO (1.7 ± 0.8 ppbv), NO_2 (17.9 ± 10.2 ppbv), and PM_{10}(0.18 ± 0.11 mg m^{-3}) in urban air in Kathmandu. Surprisingly high ratios of chemically formed secondary [HONO] to [NO_2] (up to 30%) were found, which indicates unexpectedly efficient chemical conversion of NO_2 to HONO in Kathmandu. The ratios of [HONO]/[NO_2] at night were found to be much higher than previously reported values from measurements in urban air in Europe, North America and Asia. The influences of aerosol surface, ground reactive surface, and relative humidity on NO_2-HONO chemical conversion were discussed. The high humidity, strong and low inversion layer at night, and high aerosol pollution burden in Kathmandu may explain the particularly efficient conversion of NO_2 to HONO.
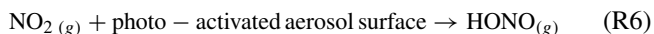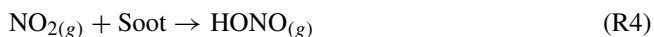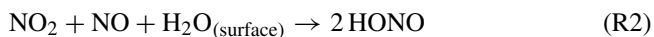
1 Introduction

Atmospheric nitrous acid (HONO) has been studied for a long time, and at a wide range of locations. It can be an important source of hydroxyl free radical (OH) in the atmosphere, especially in the morning (Lammel and Cape, 1996; Harrison et al., 1996). Despite its importance, and several decades of research, nitrous acid's formation mechanism remains unclear. Further investigation of the sources of nitrous acid in the atmosphere is important for improving our understanding of atmospheric chemistry processes.

One source of atmospheric HONO is the gas phase reaction of NO with OH (Seinfeld and Pandis, 1998; Lammel, 1999; Kleffmann, 2007). However, gas phase reactions (including NO with OH and NO_2 with peroxy or alkoxy radicals – Stockwell and Calvert, 1983) are too slow to explain the atmospheric HONO concentration. Direct emission from combustion engines is another source of HONO in the atmosphere (Kurtenbach et al., 2001; Kirchstetter et al., 1996; Wormhoudt et al., 2007; Geiger et al., 2002). Ratios of [HONO] to total [NO_x] ([NO]+[NO_2]) ranging from 0.3%–0.8% have been observed in direct emissions from vehicle engines. However, observations of [HONO]/[NO_2] ratios of a few percent in a wide range of urban atmospheres suggest that direct emission from combustion engines is probably not a major source of HONO.

Correspondence to: Y. Yu
(yyu@arb.ca.gov)

A number of heterogeneous formation mechanisms of HONO have been proposed (Reactions 1–6):

$$NO_{2(ads)} + NO_{2(ads)} + H_2O_{(surface)} \rightarrow HONO_{(g)} + HNO_{3(aq)} \quad (R1)$$

$$NO_2 + NO + H_2O_{(surface)} \rightarrow 2\,HONO \quad (R2)$$

$$NO + HNO_{3(surface)} \rightarrow HONO + NO_2 \quad (R3)$$

$$NO_{2(g)} + Soot \rightarrow HONO_{(g)} \quad (R4)$$

$$NO_{2(g)} + VOC_{(surface)} \rightarrow HONO_{(g)} \quad (R5)$$

$$NO_{2\ (g)} + photo - activated\ aerosol\ surface \rightarrow HONO_{(g)} \quad (R6)$$

Laboratory research has shown that Reactions (1–3) are heterogeneous formation processes involving NO$_x$ and water on surfaces (Finlayson-Pitts et al., 2003). Past research on the mechanisms of HONO heterogeneous reactions points to the importance of reaction surfaces, and indicates that the production efficiency of HONO depends upon the amount of water absorbed by surfaces (Finlayson-Pitts et al., 2003; Kurtenbach et al., 2001; Grassian, 2001, 2002). Nitrous acid can be formed through Reaction (1) on the surface of aerosols and the ground (Trick, 2004; Harrison and Kitto, 1994; Andrés-Hernández et al., 1996; Reisinger, 2000; Wang et al., 2003; Notholt et al., 1992a). Some studies have suggested Reaction (2) as a source of HONO in the atmosphere (Andrés-Hernández et al., 1996; Calvert et al., 1994); however, other laboratory studies and field observations (including our observation in this paper) have shown high HONO formation in the absence of NO (Alicke et al., 2002; Kleffmann et al., 1998a; Svensson et al., 1987). Reaction (2) is thus unlikely to play an important role in the atmosphere. Reaction (3) was only studied under conditions of high NO concentrations (Saliba et al., 2000, 2001), and thus not important in real atmospheric conditions with low NO concentrations.

Recently, the reaction of NO$_2$ on soot particles (Reaction 4) has been suggested to be a source of HONO in the atmosphere (Aubin and Abbatt, 2007; Alcala-Jornod et al., 2000; Nienow and Roberts, 2006; Ammann et al., 1998; Gerecke et al., 1998; Longfellow et al., 1999; Arens et al., 2001; Al-Abadleh and Grassian, 2000; Aumont et al., 1999; Grassian, 2001, 2002; Karagulian and Rossi, 2007). Soot (or black carbon) aerosols often have a loading of 1.5 to 20 $\mu g\,m^{-3}$ in urban air, mostly from anthropogenic sources, e.g., fossil fuel combustions (IPCC, 2001). The fractal and porous surface of soot provides a large contribution to the total reactive aerosol surface even when soot may have a relatively small contribution to the total aerosol mass. Studies using black carbon and soot as a substrate have demonstrated the reactive uptake of NO$_2$ and the formation of NO and HONO (Aubin and Abbatt, 2007; Kleffmann, 2007). Reaction (4) will contribute significantly to the production of atmospheric HONO only under certain conditions of high NO$_2$

concentrations and high and fresh soot loadings with large surface areas (Arens et al., 2001; Aubin and Abbatt, 2007; Kleffmann et al., 1999), and is thus not important in many real atmospheric conditions with low NO$_2$ and soot concentrations.

Reaction (5), the reactions of NO$_2$ with the adsorbed VOCs (i.e. anthrarobin, aromatics) on surfaces, is also a possible source of HONO (Arens et al., 2002; Gutzwiller et al., 2002; Lahoutifard et al. 2002).

Although high HONO levels are usually observed at night-time, atmospheric measurements, laboratory studies and model calculations have shown the enhanced formation of HONO during daytime (Stemmler et al., 2007; George et al., 2005; Gustafsson et al., 2006; Bejan et al., 2006; Rohrer et al., 2005; Liao et al., 2006a; Zhou et al., 2001; Honrath et al., 2002; Domine and Shepson, 2002; Akimoto et al., 1987; Kleffmann, 2007). It has also been shown that NO$_2$ can be efficiently reduced to form HONO under UV light on the surface of TiO$_2$, humid acid, and other organic compounds (Reaction 6) (Kleffmann, 2007; Stemmler et al., 2007, 2006; George et al., 2005; Gustafsson et al., 2006).

HONO formed in homogenous and heterogeneous reactions is released to the gas phase and accumulates during the night. Photolysis of HONO after sunrise provides a pulse of strong OH formation, which strongly influences atmospheric chemistry processes. Field measurements of HONO and its precursor NO$_2$ at locations with various aerosol loads, aerosol compositions, relative humidity, boundary layer heights and vertical transport efficiencies are thus essential for improving our understanding of the HONO formation mechanism.

Gaseous HONO in ambient air was measured for the first time by Perner and Platt (Perner and Platt, 1979) using differential optical absorption spectroscopy (DOAS). Besides the DOAS technique, a variety of other methods have been developed for the detection of HONO in the atmosphere with high sensitivity and good time resolution (Liao et al., 2006a,b; Takenaka et al., 2004; Trebs et al., 2004; Kleffmann et al., 2002; Huang et al., 2002; Vecera and Dasgupta, 1991; Heland et al., 2001). Measurements of HONO in the atmosphere have been carried out in many areas of Europe and the US. Elevated atmospheric HONO concentrations have also been detected in some Asian cities, suggesting HONO to be an important OH source in these places (Table 1). However, knowledge about HONO sources, sinks, and concentrations is almost nonexistent in South Asia. Due to the different source strengths, aerosol burdens, and the composition of aerosol and ground surfaces, HONO chemistry in South Asia is expected to have different features from what has been found in Europe or North America. For example, the average atmospheric aerosol burden in Kathmandu in winter is much higher than in European and US cities (Sharma et al., 2002; Sharma, 1997; Yu et al., 2008a; Giri et al., 2006). Moreover, strong nocturnal inversion layer (Kondo et al., 2002; Regmi et al., 2003; Panday, 2006; Panday and Prinn, 2009) and the

Table 1. HONO and NO_2 measurements in Asia.

Location	Month/Year	Type	NO_2/ppb (Mean)	HONO /ppb (Mean)	HONO/NO_2 (Mean)
Beijing/China (Hu et al., 2002)	May, Jun–Jul, Sep, Dec 2000	urban		0.8–3.1	
Beijing/China (Qin et al., 2006)	Aug–Sep 2004	urban	5–85	0.4–6.1	2%–10%
Guangzhou/China (Hu et al., 2002)	Jul, Nov 2000	urban		1.0–2.7	
Hong Kong/Hong Kong (Zhang et al., 2007)	Oct–Dec 2002	urban/ suburban		∼1–10	
Shanghai/China (Hao et al., 2006)	Oct 2004–Jan 2005	urban	5.5–75.4 (24)	0.3–6.8 (1.1)	1%–13%
Xinken/China (Su et al., 2008a,b)	Oct–Nov 2004	rural	8.2–91.4 (34.8)	0.4–3.8 (1.2)	1.4%–10.2% (4.3%)
Taichung/Taiwan (Lin et al., 2006)	Jan–Dec 2002	urban	10–46 (1.5)	0.6-4.0	
Taichung/Taiwan (Cheng et al., 2007)	Oct 2002	urban	(39.8±12)	(2.9±1.4)	
Ren-Ai/Taiwan (Cheng et al., 2007)	Oct 2002	Forest	(7.8±1.4)	(0.2±0.1)	
Seoul/South Korea (Kang et al., 2006)	Apr 2001–Feb 2002	urban		0.5–9.7 (2.8)	
Seoul/South Korea (Shon et al., 2007)	May 2004 Jun 2004	urban	(26±14) (22±11)	(1.8±1.4) (1.7±1.1)	
Yangpyung/South Korea (Shon et al., 2007)	May 2004 Jun 2004	rural	(18±9) (17±9)	(0.2±0.2) (0.6±0.8)	
Kwangju/South Korea (Park et al., 2004)	Sep–Nov 2001	Semi-urban	0–90	0.02–3.0	2%–6%
Nara/Japan (Matsumoto and Okita, 1998)	Jun 1994–May 1995	urban		0.4–1.4 (0.75)	
Sakai/Japan (Takenaka et al., 2004)	Nov–Dec 2003	urban		0.1–1.8	
Tsukuba/Japan (Kanda and Taira, 1990)	Feb 1990	rural	5–15	0.2–0.7	
Kathmandu/Nepal (this work)	Jan–Feb 2003	urban	2.9–51.6 (17.9)[1]	0.15–7.45 (1.7)[1]	1%–30% (9.5%)[1]

[1] Only nighttime data

low mixing layer height keep pollutants close to the ground, providing a large reactive ground surface for HONO formation. The high aerosol concentrations, the strong inversion layer, and the low inversion height could play an important role in the heterogeneous formation of HONO.

In this study, we present measurements of HONO and NO_2 using long path DOAS in Kathmandu, Nepal, over several weeks in 2003. As far as we are aware, this was the first study on HONO and NO_2 in the nocturnal atmosphere in South Asia. Our observations provide insights into the particular HONO chemical formation processes taking place in the Kathmandu atmosphere.

2 Experimental section

2.1 Location and instruments

We carried out a field campaign in Kathmandu in winter 2003, investigating air quality and atmospheric chemical processes. NO_x (NO, NO_2), SO_2, O_3, HONO, HCHO, PM_{10}, and meteorological parameters were measured during this period.

A home-made long-path DOAS (Chalmers University) was used to measure HONO and NO_2 in Kathmandu with a time resolution of around 5–10 min. DOAS measurements were carried out from 10 January to 11 February 2003. The measurement site (27° 43.2190′ N, 85°21.417′ E) was about 2 km east of the Kathmandu Ring Road, along the main road
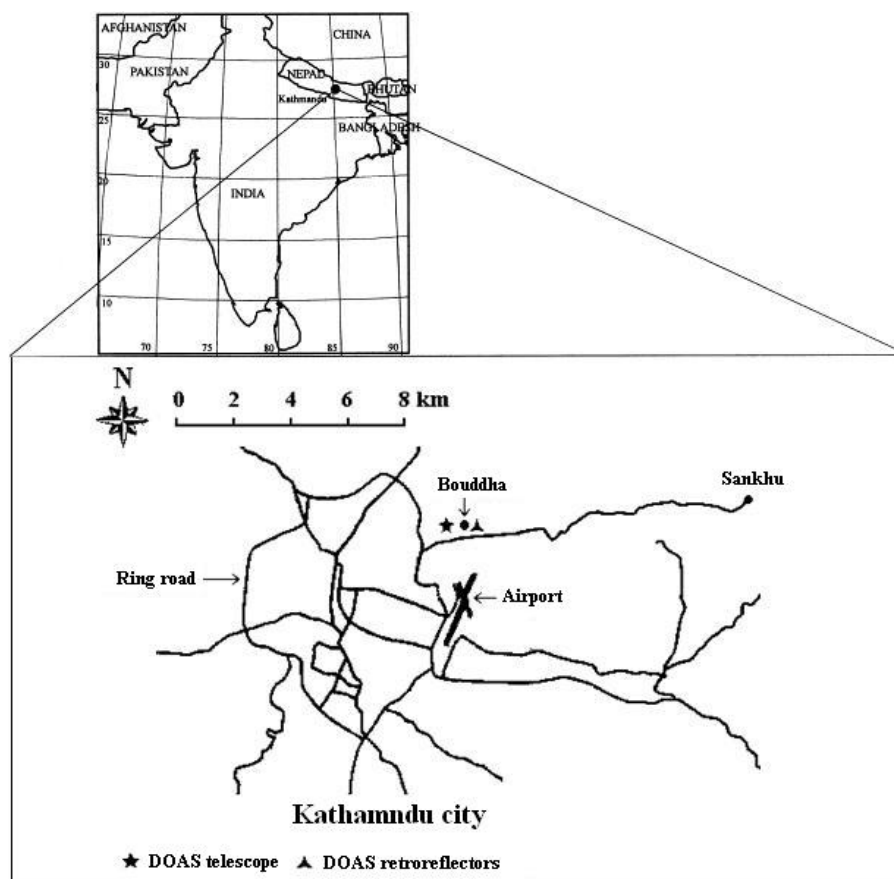
Fig. 1. Map of Kathmandu showing the measurement site.

from Kathmandu to Sankhu (Fig. 1). A DOAS telescope, a NO$_x$ analyzer (Model 42S Thermo Environmental Instruments Inc.), an O$_3$ monitor (2B Technologies), and a PM$_{10}$ aerosol monitor (TSI Dusttrak) were installed on the 5th floor of a hotel (15 m above ground). DOAS retro-reflectors were mounted at the top of a 7-story building, 25 m above ground and 957 m away from the DOAS telescope, giving a DOAS light path of 1914 m. Low buildings, roads, and some bare fields were under the light path. An automated weather station (Rainwise), which measured temperature, wind speed, wind direction, relative humidity, dew point temperature, and solar radiation, was installed on the roof of the hotel (22 m above ground) near the DOAS telescope and other instruments. Details of the DOAS instrument and the experimental sites have been described in earlier papers (Yu et al., 2008a., 2004).

In our experiments, several steps were taken before the spectral retrieval to determine concentrations of HONO, NO$_2$, and other gases. The spectra were corrected for electronic offset and light from sources other than the Xe arc lamp. The spectra were divided by a recorded halogen lamp spectrum, which only contains broadband structures, to eliminate spectral structures originating from the pixel-to-pixel

variation of the quantum yield. A digital high pass filter was used to separate narrow absorption structures from the broadband structures caused by the lamp, Rayleigh and Mie scattering, and other instrument effects. Then, a digital low pass filter was applied to reduce high frequency noise. Finally, the spectra were analyzed for NO$_2$ (cross section by Vandaele et al., 2002), HONO (cross section by Stutz et al., 2000), and HCHO (cross section by Meller and Moortgat, 2000) using a nonlinear least-squares method (Stutz and Platt, 1996) in the spectral range of 310–380 nm with a spectra resolution of 0.4 nm. The sources of errors of the measured HONO and NO$_2$ mixing ratios include the error (5% for HONO and 3% for NO$_2$) of the cross sections, the spectral fit error (less than 5%), and the experimental error of the DOAS system (5%). The total errors for the measured HONO and NO$_2$ mixing ratios are estimated to be around 9% and 8%, respectively.

2.2 Retrieval method of aerosol parameters

To investigate the role of aerosols in HONO formation, measurements of aerosol parameters such as the aerosol surface density are required, along with the ambient concentration of HONO and NO$_2$. Box and Lo (1976) developed a simple

inversion method to calculate the approximate aerosol size distribution from light attenuation. This has been further applied to calculate other aerosol parameters such as the surface density and the volume using DOAS measurements (Notholt et al., 1991, 1992a; Notholt et al., 1992b; Notholt and Raes, 1990; Flentje et al., 1997; Reisinger, 2000).

Light transmission measurements through the atmosphere can yield bulk aerosol parameters such as diameters, number density, total surface, and total volume of particles (Livingston and Russell, 1989). In Kathmandu, we used the DOAS system to measure the light transmission, aerosol parameters and trace gas concentrations simultaneously in the same volume of air.

The spectra were recorded in the 250–390 nm range. The range of 330 nm to 390 nm was used to retrieve concentrations of HONO, NO$_2$ and aerosol parameters simultaneously. A background spectrum was recorded over a 1 m optical path using retroreflectors. Given the concentrations of all gases provided by the DOAS spectra retrieval processes (SO$_2$, O$_3$, NO$_2$, HONO, and HCHO), the optical depth (τ) at wavelength λ can be calculated according to Eq. (1).

$$\tau(\lambda) = -\ln\left(\frac{I(\lambda)}{I_0(\lambda)}\right) \qquad (1)$$

Here $I(\lambda)$ is the light intensity at the end of the full path length while $I_0(\lambda)$ is the background light intensity at 1 m path length. Inversion of the optical depth is performed using a look-up table (Box and Lo, 1976). The spectral fit at 330–390 nm region was based on an assumed exponential wavelength-dependent function for optical depth:

$$\tau_{\exp}(\lambda) = \beta \cdot e^{-a \cdot \lambda} - k \qquad (2)$$

where $\tau_{\exp}(\lambda)$ is the optical depth, α and β are the fitting parameters, and k is the offset constant. The offset k must be considered because of instrument factors such as the reflecting ratio of retroreflectors.

Using α, β, and the pre-calculated tables of Box and Lo (1976), values of a and b can be obtained for the calculation of Deirmendjian's particles size distribution $n(r)$ (Box and Lo, 1976; Notholt and Raes, 1990; Notholt et al., 1992b, 1991):

$$n(r) = \frac{1}{2} \cdot a \cdot b^3 \cdot r^2 \cdot e^{-b \cdot r} \qquad (3)$$

where r is the particle radius, and the constants a and b are specified for different particles types.

By using the same method as described by Notholt et al. (1992a) but with a narrower spectral range, we calculated the aerosol size distribution and further obtained the total number, surface density and the volume of aerosols in time intervals of 5–10 min.

Our light attenuation retrieval processes give a large uncertainty of aerosol parameters. Errors in this method have been extensively discussed by others (Andres-Hernandez et al., 1996; Notholt et al., 1992a; Notholt and Raes, 1990; Box and Lo, 1976). The total error of our results was estimated to be 55%. The sources are: (1) The unknown refractive index of the aerosols (we have tested different indices from 1.33 to 1.70. Trends with different indices are similar but with different values) could contribute an uncertainty as large as 50% (Box and Lo, 1976); (2) The relatively narrow spectral range compared to the application by Notholt et al. (1992a) gave 20% uncertainty as reported by Reisinger (2000); (3) The deviation of the true aerosol size distribution from the calculated results by the model (Deirmendjian's particle size distribution) could introduce an additional uncertainty; (4) The consistency of the lamp intensity and DOAS mechanical stability is sufficient during a time period of a few weeks but with an uncertainty of 10% (Andres-Hernandez et al., 1996; Notholt et al., 1992a).

With such limitations, the results of aerosol parameters are only approximations of the true aerosol situation. Nevertheless, the retrieval results of aerosol surface and volume (assuming a refractive index $n = 1.5$ – Yu et al., 2008b) agree well with the trends seen in our PM$_{10}$ data (Fig. 2), which confirms the reliability of our calculated aerosol parameters.

The aerosol mass in this study was calculated from a typical urban aerosol density of 1.4 ± 0.5 g cm^{-3} (Pitz et al., 2003) and the measured aerosol volume ($\sim 1 \times 10^2$ μm^3 cm^{-3}, 00:00–04:00 in Kathmandu in Fig. 2). We found the average atmospheric aerosol mass concentration at midnight in Kathmandu to be 140 ± 50 μg m^{-3}. However, light attenuation only gives the aerosol information (aerosol diameters, surface and volume) for fine particles with diameters smaller than 1 μm. Assuming a PM$_1$/PM$_{10}$ mass ratio of 50% in urban air (Vallius et al., 2000; Ehrlich et al., 2007; Ariola et al., 2006; Spindler et al., 2004; Labban et al., 2004; Li and Lin, 2002; Gomiscek et al., 2004; Liu et al., 2004), the calculated aerosol mass by light attenuation is in agreement with our measured PM$_{10}$ values.

3 Results and discussion

3.1 Time series of HONO, other pollutants and meteorological data

Continuous measurements were carried out during January and February, 2003. Figure 3 shows, as an example from our one-month observation, the behavior of HONO, NO$_x$, [HONO]/[NO$_2$], PM$_{10}$, and meteorological parameters (radiation, wind speed and wind direction) during a four day period. The wind direction becomes unimportant as wind speeds drop to zero during our observation. NO$_2$ and HONO measurements by the long path DOAS show gaps every morning and on some evenings due to heavy fog and smog.

The concentration of NO had two peaks (with values as high as 60 ppb) at 07:00–08:00 and 19:00–20:00, respectively, and remained low (a few ppb except for short duration plumes) at night. As our campaign was at a time of
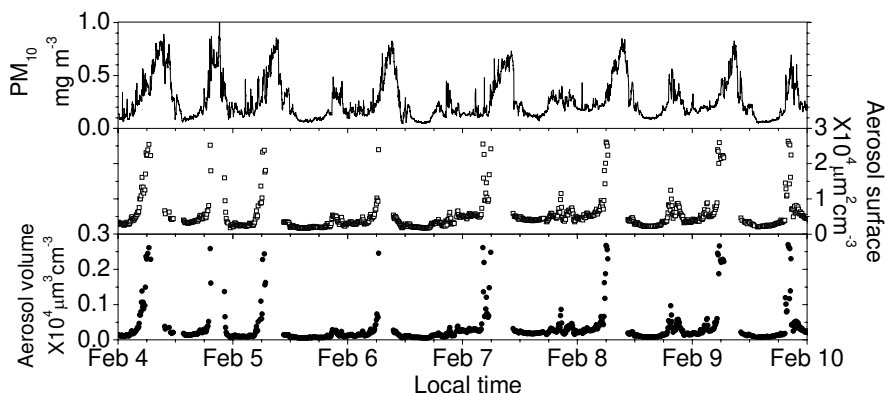
Fig. 2. PM$_{10}$, aerosol surface and volume measured in Kathmandu, 2003.
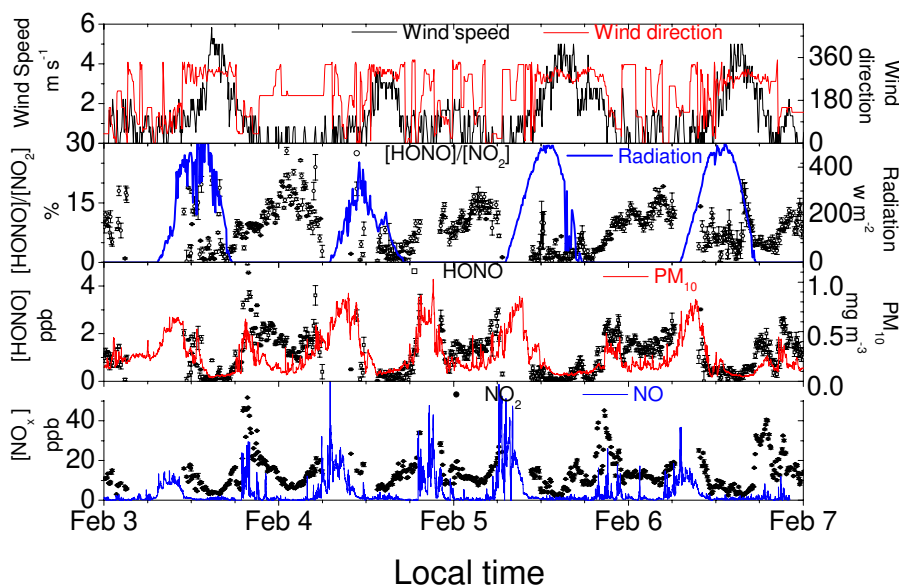
Fig. 3. Behavior of [NO$_2$], [HONO], [HONO]/[NO$_2$], PM$_{10}$, and meteorological parameters (wind speed, wind direction, and solar radiation) during 3–7 February in Kathmandu urban air. The error bars are 1σ standard deviation.

considerable political instability in Nepal, with frequent ve-hicle searches at night, night-time driving was quite low and thus the night-time sources of NO were limited. Peaks in NO$_2$ appeared concurrently with the NO peaks at 07:00–08:00 and 19:00–20:00. NO$_2$ values were around 10–20 ppb at night, and started to increase around 03:00–04:00. HONO concentrations climbed to several ppb after sunset and then decreased to around 1–1.5 ppb. It increased again after 03:00. PM$_{10}$ shows elevated values (up to 1 mg m^{-3}) during the morning and evening. The diurnal variation of the observed wind pattern shows a long calm period from sunset ($\sim$18:00) until around 10:00 each day. The morning and evening peaks in NO$_x$ and PM$_{10}$ did not correspond to rush hour alone. In particular, the evening peaks started after the rush hour. The timing of pollutant peaks in Kathmandu is determined

by the valley's ventilation pattern (Panday, 2006; Panday and Prinn, 2009). The correlation of HONO with NO$_2$ and PM$_{10}$ (especially after sunset) in Fig. 3 suggests three possi-bilities: (1) the same emission source; (2) chemical conver-sion of NO$_2$ to HONO associated with aerosols; (3) all three species have their sources near the ground (not necessarily the same sources). The HONO formation mechanism will be discussed in later sections.

Table 2 shows several pollutants measured in Kath-mandu's urban air. Elevated mixing ratios of HONO (up to $\sim$7.5 ppbv) were observed during the whole measurement period. The elevated HONO concentrations in the presence of high [NO], [NO$_2$] and PM$_{10}$ values right after sunset ap-pear to be the result of several processes: (1) direct emission at evening rush hours; (2) decrease of boundary layer height

Table 2. Pollutants in Kathmandu urban air.

| Pollutant	Mean (ppbv)[1]						Minimum (ppbv)[1]	Maximum (ppbv)[1]
	Total	SD	Day[2]	SD	Night[3]	SD		
NO$_2$	14.14	9.77	8.59	5.65	17.94	10.23	0.692	70.11
NO	3.16	6.41	4.41	7.51	2.17	5.19	0.011	162.72
HONO	1.55	1.57	0.351	0.444	1.736	0.804	0.026	7.45
PM$_{10}$	0.197	0.153	0.216	0.193	0.182	0.109	0.011	1.27

[1] PM$_{10}$ unit is mg m^{-3}; [2] daytime: 07:00–18:00; [3] nocturnal: 18:00–07:00

after sunset; (3) insufficient dispersion of polluted air mass due to reduced wind speed; (4) the ceasing of photolysis of NO$_2$ and HONO after sunset.

3.2 High atmospheric [HONO]/[NO$_2$] values in Kathmandu at night

In many field studies, the value of [HONO]/[NO$_2$] is used as an index to estimate the efficiency of heterogeneous NO$_2$-HONO conversion because it is less influenced by transport processes than individual concentrations. Figure 3 shows that in Kathmandu, [HONO]/ [NO$_2$] climbed after sunset and reached its highest point around 02:00–03:00. The highest [HONO]/[NO$_2$] values during 3 to 7 February were from 15% to 28% between 00:00 and 03:00. The diurnally repeating trends of [NO$_x$], [HONO] and [HONO]/[NO$_2$] are most likely due to diurnally repeating wind profiles, emission sources, boundary layer dynamics and chemical processes. During afternoon rush hours and other plume events (around 19:00, 20:00, and 21:00), [HONO] followed the same pattern as [NO$_2$] (Fig. 3). However, during those times a lower [HONO]/[NO$_2$] value was observed compared to a few hours later, similar to the observation in Houston (Stutz et al., 2004). It is likely that conversion of NO$_2$ to HONO in relatively freshly polluted air has not proceeded as far as in the aged air in this period.

A scatter plot of nocturnal [HONO] and [NO$_2$] is shown in Fig. 4. The regression coefficient, maximum and minimum ratio of [HONO] to [NO$_2$] were 0.081, 0.30 and 0.008, respectively. The maximum [HONO]/[NO$_2$] ratio (30%) found in our observation is, to our knowledge, the highest reported atmospheric HONO to NO$_2$ ratio, with the exception of daytime findings in and above snow (Zhou et al., 2001). The high ratios of [HONO]/[NO$_2$] in Kathmandu at night indicate high HONO direct emissions, or highly efficient NO$_2$ to HONO chemical conversion, or both. In the next sections, we discuss the contribution of direct emissions and chemical processes separately.
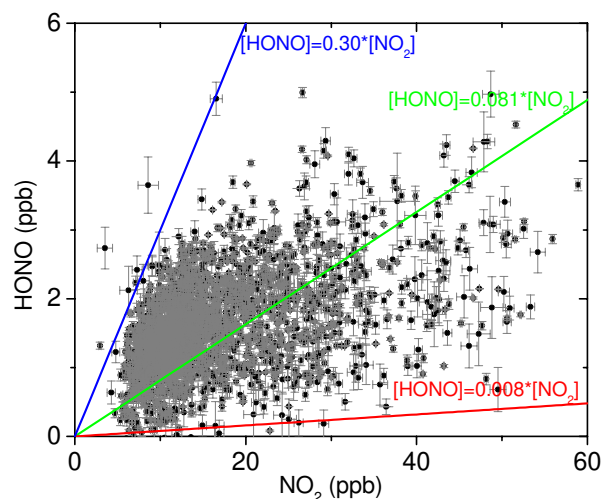
Fig. 4. [HONO] vs. [NO$_2$] in the nocturnal atmospheric boundary layer at an urban site of Kathmandu. The error bars are 1σ standard deviation.

3.3 Contribution of direct emissions to the observed HONO

It is necessary to separate HONO formed by chemical reactions from HONO that is directly emitted (mainly from vehicles; the contribution from industrial combustion processes is not clear). No previous study reported the ratio of [HONO]/[NO$_x$] in emissions in Kathmandu. The highest reported average emission ratio anywhere in the recent literature was (0.8±0.1) % (Kurtenbach et al., 2001). Based on the observation of HONO, NO$_x$ and [HONO]/[NO$_2$] in this study, it is believed that direct emission was not the major source of HONO in Kathmandu. The reasons are: first, the [HONO]/[NO$_2$] ratio was low (around a few %) after sunset when emissions were high and high NO$_x$ concentrations were observed. Second, NO$_x$ concentrations were low in the middle night, ruling out the possibility of direct emissions as the major source of HONO. Third, as we see in Fig. 4, the

minimum value of [HONO]/[NO$_2$] was $\sim 0.8\%$; corresponding to the maximum possible contribution by HONO direct emissions.

The high value of [HONO]/[NO$_2$] (upto 20% during most nights, exceeding 25% during some nights, and reaching a maximum of 30% during one night) is thus mostly due to secondary HONO.

This maximum ratio of 30% is substantially higher than the previously observed ratios at other urban and suburban sites in Europe, North America and Asia (i.e., 1–12% reported by Lammel and Cape (1996), 19% reported by Wang et al. (2003) during dust storms, and 1–13% around Asia – Qin et al., 2006; Park et al., 2004; Hao et al., 2006).

3.4 NO$_2$-HONO chemical conversion and correlation studies

The contribution by NO to the formation of HONO through Reactions (2–3) could be ruled out for Kathmandu late at night because of the low NO concentrations. According to HONO formation mechanisms (Reactions 1 to 6 in the introduction), the major source of HONO in the nocturnal air in Kathmandu was the NO$_2$ to HONO chemical conversion through heterogeneous reactions (i.e. Reactions 1, 4, and 5).

HONO formation has been found to be a first order reaction in NO$_2$ (Finlayson-Pitts et al., 2003; Kleffmann et al., 1998a). It depends on the surface absorbed water, and increases as the reactive surface to air volume ratio (S/V) increases (Stutz et al., 2004; Trick, 2004). The value of S/V is determined by a combination of the aerosol surface, ground reactive surface and the influence of vertical mixing (Febo et al., 1996; Trick, 2004). Here we investigate S/V ratio and relative humidity in the nocturnal atmosphere in Kathmandu and their influence on HONO formation.

The correlation of HONO with other pollutants in Fig. 3 indicates the following. (1) the presence of all the compounds in the same air mass; (2) a chemical conversion of NO$_2$ to HONO associated with aerosols; (3) all three species have their sources near the ground (not necessarily the same sources). In order to investigate the efficiency of NO$_2$ to HONO chemical conversion without the influence of other processes (i.e. transport), we study the correlation of [HONO]/ [NO$_2$] instead of [HONO] to the other parameters.

3.4.1 Aerosol surface and ground reactive surface

Long path DOAS measurements can provide information about aerosol surface-to-air volume ratios (see Sect. 2). The ground reactive surface area density is defined in this paper as the inverse value of the mixing layer height (H^{-1}) (Harrison et al., 1996). We use average mixing layer heights from Sonic Detection & Ranging (SODAR) measurements (Panday, 2006). The average measured mixing layer height deceased from 12:00 (800 m) until 00:00 (120 m), and then re-

mained approximately constant (120 m) from 00:00 to 06:00. It has to be noted that mixing layer height measurements by SODAR are less accurate at night than during the day.

The porosity of aerosols and the roughness of the ground surface were not considered in this study. The area densities of aerosol surfaces and ground reactive surface might be higher (up to 10 times) (Lammel and Cape, 1996; Andrés-Hernández et al., 1996) than the values calculated from light attenuation and estimation by mixing layer height, respectively.

Figure 5a shows the behaviors of [HONO]/[NO$_2$], and during a selected night. The black line in Fig. 5a is the combination of the two surface area densities. [HONO]/[NO$_2$] increased after sunset and remained relatively constant after 00:00, then decreased after 03:00. $\left(\frac{S}{V}\right)_{\text{aerosol}}$ increased quickly after sunset for a short period (17:00–19:00), and then stayed nearly constant until 03:00. $\left(\frac{S}{V}\right)_{\text{aerosol}}$, as well as PM$_{10}$, dramatically increased after 03:00. The change of $\left(\frac{S}{V}\right)_{\text{aerosol}}$ has a positive correlation with [HONO]/[NO$_2$] right after sunset. However, for the period of 17:00 to 03:00, $\left(\frac{S}{V}\right)_{\text{aerosol}}$ has a poor correlation ($R^2 = 0.33$) to [HONO]/[NO$_2$] (see Fig. 5b), which disagree with observations in some field measurements elsewhere (Notholt et al., 1992a; Reisinger, 2000). It is interesting that $\left(\frac{S}{V}\right)_{\text{ground}}$ shows good correlation with [HONO]/[NO$_2$] ($R^2 = 0.93$) for the whole night except between 03:00 and 06:00 in Fig. 5b. The good correlation between [HONO]/[NO$_2$] and $\left(\frac{S}{V}\right)_{\text{ground}}$ indicates that the NO$_2$ heterogeneous reaction on the ground reactive surface was a major source of HONO in Kathmandu. Our observation of ground reactive surface as a source of atmospheric nitrous acid is consistent with other field observations (Harrison and Kitto, 1994; Harrison et al., 1996; Kleffmann et al., 2003; Vogel et al., 2003).

Although the general correlation of [HONO]/[NO$_2$] with $\left(\frac{S}{V}\right)_{\text{aerosol}}$ was poor, the positive correlation in the early hours after sunset (17:00-19:00) points to the possible contribution of aerosols to HONO formation under certain conditions. Recently many researchers have reported the fast conversion of NO$_2$ on fresh soot surface to form HONO (Reaction 4). Since the soot surface is shown to rapidly deactivate as the reaction proceeds, it is believed to be an insignificant source of HONO in the real atmosphere. However, the aerosol concentrations in Kathmandu air are much higher than in those cities, where research on this topic was carried out. It is thus worthy to investigate the potential impact of soot on HONO formation in Kathmandu atmosphere.

Although aerosol chemical properties in the Kathmandu urban area were not provided by our measurements, literature and many reports in local newspapers suggest that large amounts of soot are often present in the winter Kathmandu urban air. Some researchers have attributed the dark haze over Kathmandu valley to the presence of soot particles (Sapkota and Dhaubhadel, 2002). Others investigated the aerosol chemical properties in Nagarkot, at the rim of the
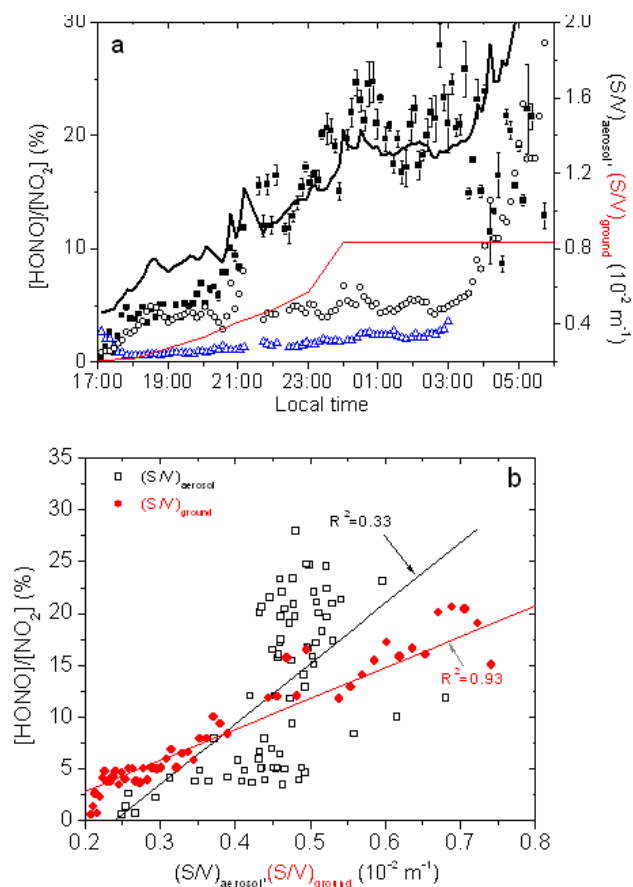
Fig. 5. (a) Observed [HONO]/[NO_2] (square), aerosol surface density (open circle), calculated [HONO]/[NO_2] due to Reaction (4) (blue triangle), ground reactive surface density (red line) and total surface density or (S/V)aerosol + (S/V)ground (black line) at 21–22 January 2003. **(b)** Linear correlations of [HONO]/[NO_2] to aerosol surface density and ground reactive surface density.

Kathmandu valley, and found that the aerosol featured a dominant contribution from carbon, likely from fuel combustion and biomass burning processes in the Kathmandu valley (Carrico et al., 2003). More recent research shows elevated levels of black carbon and organic carbon in the Kathmandu urban air from September 2004 to August 2005 (Adhikary et al., 2007; Ramanathan et al., 2007). It has been estimated that brick-kilns are responsible for about 28% of annual PM_{10} emissions in the valley, almost all of which is concentrated during the winter months (World Bank, 1997). The operation of 125 brick kilns in the Kathmandu valley during the dry season from December to April evidently contributes to the aerosol pollution, including black carbon emissions (Dhakal, 2003; Adhikary et al., 2007).

In this study, we used an integrated HONO formation rate for unit surface area of soot particles, 1.3×10^{14} molecules cm^{-2} (average of the values provided by Aubin and Abbatt, 2007; Kleffmann and Wiesen, 2005; Kirchner et al., 2000). By assuming that all observed parti-

cles were soot, we got an upper estimate of the average soot particle surface. The calculated [HONO]/[NO_2] values corresponding to Reaction (4) are plotted in Fig. 5a (triangles). The maximum HONO formed by NO_2 conversion on soot is found to be $\sim (0.3 \pm 0.2)$ ppb, which corresponds to a [HONO]/[NO_2] ratio of $3 \pm 2\%$. Compared to our observations during most parts of the nights, this is a very small contribution. However, for the early hours after sunset (17:00–19:00), the majority of the observed [HONO]/[NO_2] ratio (below 5%) could come from Reaction (4) on soot particles. Despite the fact that soot may play a role in NO_2-HONO conversion in Kathmandu right after sunset based on our calculation, we should note that: (1) there is inadequate information about aerosol chemical composition; (2) the contribution of this process to total nocturnal atmospheric HONO formation is most likely limited.
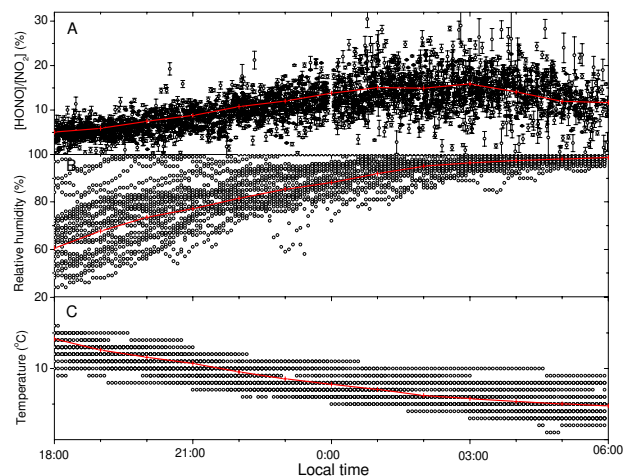
3.4.2 Relative humidity (RH)

The RH dependent HONO formation has been studied in laboratory research (Harrison and Collins, 1998) and in field observations (Stutz et al., 2004). Syomin and Finlayson-Pitts (2003) have studied the decomposition of HONO under different RH conditions. The RH in the winter of Kathmandu increased from a sunset value of $\sim$60% to $\sim$100% by 03:00 and remained close to 100% until sunrise during most nights. Figure 6 (panels A, B) shows the time series of [HONO]/[NO_2], RH, and temperature in Kathmandu during the entire observation period. The red lines indicate the mean values. While the increasing RH (from 60% to 95%) accompanied increasing [HONO]/[NO_2], [HONO]/[NO_2] values decreased after RH reached $\sim$100%.

However, the correlation of [HONO]/[NO_2] with RH in Fig. 6 might not be a proof for the humidity dependence of HONO formation in Kathmandu atmosphere. The increasing RH after sunset was the result of the decreasing temperature (panel C in Fig. 6). Meanwhile, the increasing [HONO]/[NO_2] during the night was due to the combination of ceasing photochemistry, heterogeneous formation and a decreasing boundary layer height. Simultaneous increase of RH and [HONO]/[NO_2] as shown in Fig. 6 might be two independent processes. In order to test the influence of RH on the NO_2-HONO conversion reactions, we study the average HONO formation rate constant during the night against the average humidity.

HONO formation has been found to be first order in NO_2, dependent on the surface absorbed water, and increasing with aerosol surface to air volume ratio (Kleffmann et al., 1998b; Sumner et al., 2004; Finlayson-Pitts et al., 2003).

We can thus use Eq. (4) to describe the HONO formation at night:

$$\frac{d[\text{HONO}]}{dt} = k_{\text{RH}} \times [\text{NO}_2] \times \frac{S}{V} \qquad (4)$$

Fig. 6. [HONO]/[NO$_2$], relative humidity, and temperature in the nocturnal Kathmandu atmosphere during the whole observation period. Lines with plus marks show average values.

Fig. 7. Normalized HONO formation rate constants decrease with the increasing RH. Red open circles are individual HONO formation values of each night. Black dots are average values of HONO formation in RH range of 65–75%, 75–85%, 85–95% and 95–100%. Error bars are the standard deviations.
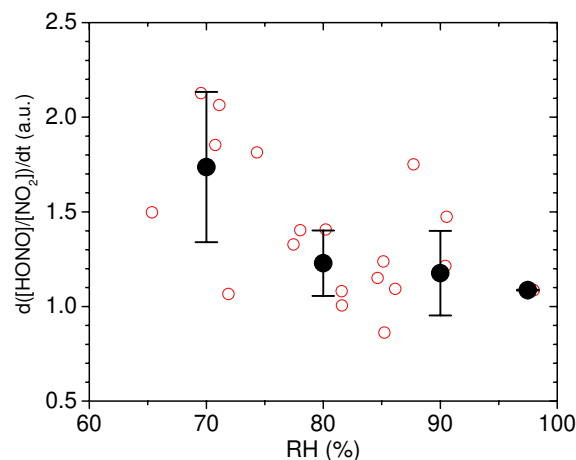
k_{RH} is an assumed RH dependant HONO formation rate constant.

Here we determine the HONO formation by assuming a linear increase of its mixing ratio during the time period of 18:00–00:00 in Kathmandu air. The estimation of the HONO formation rate constant in each individual night is based on the equation introduced by Alicke et al. (2002):

$$k_{RH} = \frac{[HONO]_{t_2} - [HONO]_{t_1}}{(t_2 - t_1)[NO_2]_{night}\frac{S}{V}} \tag{5}$$

The average nighttime (18:00–00:00) HONO formation rate is (0.014 ± 0.004) (ppb HONO per hour per ppb NO$_2$) during our observation period, which is slightly higher than the observations in Milan (Alicke et al. 2002). The HONO formation rate constant is normalized by the S/V, and then plotted against the average RH value of each individual night (see Fig. 7). The HONO formation evidently decreases as RH increases from 65–100% during the night in Kathmandu. The HONO formation in RH range of 95–100% is only about half of the value in RH range of 65–75%.

This negative RH dependence of HONO formation in our observations is most likely due to HONO lost in the growing aqueous layer on the ground. The water adsorption on the ground surface can be determined by BET isotherm. The number of monolayers formed by absorbed water on various surfaces increases rapidly when RH reaches 60% (Sumner et al., 2004; Lammel, 1999). Lammel (1999) had reported that the water coverage of various materials (stone, soil, and vegetation) increases dramatically (equivalent to up to 100 monolayers) when RH is over 95%. A surface with a RH of over 95% is classified as an "aqueous" surface. Such

an "aqueous" surface affects the reaction efficiency of NO$_2$-HONO conversion (Stutz et al., 2004; Lammel, 1999), which is in accordance with our observation.

The water uptake processes can take place on the ground surface (major HONO formation source in this paper) as well as aerosol surfaces. As many earlier papers reported, water droplets (on ground or aerosol) at a RH of over 96% play a role in the HONO sink, leading to lower [HONO]/[NO$_2$] values, which is in agreement with our observation (Lammel and Perner, 1988; Zhou et al., 2007; He et al., 2006; Acker et al., 2005, 2001; Lammel, 1999).

4   Conclusions

Measurements of NO$_x$, HONO, PM$_{10}$, surface density, and meteorological parameters in winter in Kathmandu were presented. To our knowledge, this was the first time that HONO was measured in South Asia.

Very high values of chemically formed HONO to NO$_2$ ratios were found (up to 30%), which is higher than any other previous atmospheric observations that we are aware of.

We believe that direct emissions and heterogeneous reactions involving NO are not the major sources of HONO in Kathmandu's nocturnal atmosphere. NO$_2$ heterogeneous chemical processes appear to be responsible for the high and periodic HONO levels under the conditions of high aerosol pollution burden, strong inversion, and high humidity. Kathmandu's very low nocturnal mixing layer height provides a large reactive surface density for HONO formation through NO$_2$ heterogeneous reaction, which is confirmed by the good correlation of ground reactive surface area density and [HONO]/[NO$_2$] values.

The high relative humidity found in Kathmandu at night provides efficient water uptake on reactive surfaces. When the relative humidity exceeds 96% in the early morning, water condenses on aerosol and ground to form water droplets, which appears to be a sink for gaseous HONO even before sunrise.

Edited by: M. Ammann

References

Acker, K., Möller, D., Wieprecht, W., Auel, R., Kalass, D., and Tscherwenka, W.: Nitrous and nitric acid measurements inside and outside of clouds at Mt. Brocken, Water Air Soil Poll., 130, 331–336, 2001.

Acker, K., Möller, D., Auel, R., Wieprecht, W., and Kalass, D.: Concentrations of nitrous acid, nitric acid, nitrite and nitrate in the gas and aerosol phase at a site in the emission zone during ESCOMPTE 2001 experiment, Atmos. Res., 74, 507–524, 2005.

Adhikary, B., Carmichael, G. R., Tang, Y., Leung, L. R., Qian, Y., Schauer, J. J., Stone, E. A., Ramanathan, V., and Ramana, M. V.: Characterization of the seasonal cycle of south Asian aerosols: A regional-scale modeling analysis, J. Geophys. Res., 112, D22S22, doi:10.1029/2006JD008143, 2007.

Akimoto, H., Takagi, H., and Sakamaki, F.: Photoenhancement of the Nitrous Acid Formation in the Surface Reaction of Nitrogen Dioxide and Water Vapor: Extra Radical Source in Smog Chamber Experiments, Int. J. Chem. Kinet., 19, 539–551, 1987.

Al-Abadleh, H. A. and Grassian, V. H.: Heterogeneous reaction of NO$_2$ on hexane soot: A Knudsen cell and FT-IR study, J. Phys. Chem. A, 104, 11926–11933, 2000.

Alcala-Jornod, C., van den Bergh, H., and Rossi, M. J.: Reactivity of NO$_2$ and H$_2$O on soot generated in the laboratory: a diffusion tube study at ambient temperature, Phys. Chem. Chem. Phys., 2, 5584–5593, 2000.

Alicke, B., Platt, U., and Stutz, J.: Impact of nitrous acid photolysis on the total hydroxyl radical budget during the Limitation of Oxidant Production/Pianura Padana Produzione di Ozono study in Milan, J. Geophys. Res., 107, 8196, doi:10.1029/2000JD000075, 2002.

Ammann, M., Kalberer, M., Jost, D. T., Tobler, L., Rössler, E., Piguet, D., Gäggeler, H. W., and Baltensperger, U.: Heterogeneous production of nitrous acid on soot in polluted air masses, Nature, 395, 157–160, 1998.

Andrés-Hernández, M. D., Notholt, J., Hjorth, J., and Schrems, O.: A DOAS study on the origin of nitrous acid at urban and non-urban sites, Atmos. Environ., 30, 175–180, 1996.

Antognozzi, M., Humphris, A. D. L., and Miles, M. J.: Observation of molecular layering in a confined water film and study of the layers viscoelastic properties, Appl. Phys. Lett., 78, 300–302, 2001.

Arens, F., Gutzwiller, L., Baltensperger, U., Gäggeler, H. W., and Ammann, M.: Heterogeneous reaction of NO$_2$ on diesel soot particles, Environ. Sci. Technol., 35, 2191–2199, 2001.

Arens, F., Gutzwiller, L., Gäggeler, H. W., and Ammann, M.: The reaction of NO$_2$ with solid anthrarobin (1,2,10-trihydroxy-anthracene), Phys. Chem. Chem. Phys., 4, 3684–3690, 2002.

Ariola, V., D'Alessandro, A., Lucarelli, F., Marcazzan, G., Mazzei, F., Nava, S., Garcia-Orellana, I., Prati, P., Valli, G., Vecchi, R., and Zucchiatti, A.: Elemental characterization of PM10, PM2.5 and PM1 in the town of Genoa (Italy), Chemosphere, 62, 226–232, 2006.

Aubin, D. G., and Abbatt, J. P.: Interaction of NO$_2$ with hydrocarbon soot: Focus on HONO yield, surface modification, and mechanism, J. Phys. Chem. A, 111, 6263–6273, 2007.

Aumont, B., Madronich, S., Ammann, M., Kalberer, M., Baltensperger, U., Hauglustaine, D., and Brocheton, F.: On the NO$_2$ plus soot reaction in the atmosphere, J. Geophys. Res., 104, 1729–1736, 1999.

Beine, H. J., Amoroso, A., Domin, F., King, M. D., Nardino, M., Ianniello, A., and France, J. L.: Surprisingly small HONO emissions from snow surfaces at Browning Pass, Antarctica, Atmos. Chem. Phys., 6, 2569–2580, 2006,
http://www.atmos-chem-phys.net/6/2569/2006/.

Bejan, I., Abd El Aal, Y., Barnes, I., Benter, T., Bohn, B., Wiesen, P., and Kleffmann, J.: The photolysis of ortho-nitrophenols: a new gas phase source of HONO, Phys. Chem. Chem. Phys., 8, 2028–2035, 2006.

Box, M. A. and Lo, S. Y.: Approximate determination of aerosol size distributions, J. Appl. Meteorol., 15, 1068–1076, 1976.

Carrico, C. M., Bergin, M. H., Shrestha, A. B., Dibb, J. E., Gomes, L., and Harris, J. M.: The importance of carbon and mineral dust to seasonal aerosol properties in the Nepal Himalaya, Atmos. Environ., 37, 2811–2824, 2003.

Calvert, J. G., Yarwood, G., and Dunker A.M.: An evaluation of the mechanism of nitrous acid formation in the urban atmosphere, Res. Chem. Interm., 20, 463–502, 1994.

Cheng, M. T., Horng, C. L., and Lin, Y. C.: Characteristics of atmospheric aerosol and acidic gases from urban and forest sites in central Taiwan, Bull. Environ. Contamin. Toxicol., 79, 674–677, 2007.

Domine, F. and Shepson, P. B.: Air-snow interactions and atmospheric chemistry, Science, 297, 1506–1510, 2002.

Ehrlich, C., Noll, G., Kalkoff, W. D., Baumbach, G., and Dreiseidler, A.: PM$_{10}$, PM$_{2.5}$ and PM$_{1.0}$ – Emissions from industrial plants – Results from measurement programmes in Germany, Atmos. Environ., 41, 6236–6254, 2007.

Febo, A., Perrino, C., and Allegrini, I.: Measurement of nitrous acid in Milan, Italy, by DOAS and diffusion denuders, Atmos. Environ., 30, 3599–3609, 1996.

Finlayson-Pitts, B. J., and Pitts, J. N., Jr.: Chemistry of the upper and lower atmosphere – theory, experiments, and applications, Academic Press, San Diego, USA, 969 pp., 2000.

Finlayson-Pitts, B. J., Wingen, L. M., Sumner, A. L., Syomin, D., and Ramazan, K. A.: The Heterogeneous hydrolysis of NO$_2$ in laboratory systems and in outdoor and indoor atmospheres: an integrated mechanism, Phys. Chem. Chem. Phys., 5, 223–242, 2003.

Flentje, H., Dubois, R., Heintzenberg, J., and Karbach, H. J.: Retrieval of aerosol properties from boundary layer extinction measurements with a DOAS system, Geophys. Res. Lett., 24, 2019–2022, 1997.

Geiger, H., Kleffmann, J., and Wiesen, P.: Smog chamber studies on the influence of diesel exhaust on photosmog formation, Atmos. Environ., 36, 1737–1747, 2002.

George, C., Strekowski, R. S., Kleffmann, J., Stemmler, K., and Ammann, M.: Photoenhanced uptake of gaseous NO$_2$ on solid-organic compounds: a photochemical source of HONO?, Faraday Discuss., 130, 195–210, 2005.

Gerecke, A., Thielmann, A., Gutzwiller, L., and Rossi, M. J.: The chemical kinetics of HONO formation resulting from heterogeneous interaction of NO$_2$ with flame soot, Geophys. Res. Lett., 25, 2453–2456, 1998.

Giri, D., Murthy, V. K., Adhikary, P. R., and Khanal, S. N.: Ambient air quality of Kathmandu Valley as reflected by atmospheric particulate matter concentrations (PM$_{10}$), Int. J. Environ. Sci. Tech., 3, 403–410, 2006.

Gomiscek, B., Hauck, H., Stopper, S., and Preining, O.: Spatial and temporal variations of PM$_1$, PM$_{2.5}$, PM$_{10}$ and particle number concentration during the AUPHEP-project, Atmos. Environ., 38, 3917–3934, 2004.

Grassian, V. H.: Heterogeneous uptake and reaction of nitrogen oxides and volatile organic compounds on the surface of atmospheric particles including oxides, carbonates, soot and mineral dust: implications for the chemical balance of the troposphere, Int. Rev. Phys. Chem., 20, 467–548, 2001.

Grassian, V. H.: Chemical reactions of nitrogen oxides on the surface of oxide, carbonate, soot and mineral dust particles: implications for the chemical balance of the troposphere, J. Phys. Chem. A, 106, 860–877, 2002.

Gustafsson, R. J., Orlov, A., Badger, C. L., Griffiths, P. T., Cox, R. A., and Lambert, R. M.: A comprehensive evaluation of water uptake on atmospherically relevant mineral surfaces: DRIFT spectroscopy, thermogravimetric analysis and aerosol growth measurements, Atmos. Chem. Phys., 5, 3415–3421, 2005, http://www.atmos-chem-phys.net/5/3415/2005/.

Gustafsson, R. J., Orlov, A., Griffiths, P. T., Cox, R. A., and Lambert, R. M.: Reduction of NO2 to nitrous acid on illuminated titanium dioxide aerosol surfaces: implications for photocatalysis and atmospheric chemistry, Chem. Commun., 3936–3938, 2006.

Hao, N., Zhou, B., Chen, D., and Chen, L. M.: Observations of nitrous acid and its relative humidity dependence in Shanghai, J. Environ. Sci., 18, 910–915, 2006.

Harrison, R. M. and Kitto, A.-M. N.: Envidence for a surface source of atmospheric nitrous acid, Atmos. Environ., 28, 1089–1094, 1994.

Harrison, R. M., Peak, J. D., and Collins, G. M.: Tropospheric cycle of nitrous acid, J. Geophys. Res., 101, 14429–14439, 1996.

Harrison, R. M. and Collins, G. M.: Measurements of reaction coefficients of NO$_2$ and HONO on aerosol particles, J. Atmos. Chem., 30, 397–406, 1998.

He, Y., Zhou, X., Hou, J., Gao, H., and Bertman, S. B.: Importance of dew in controlling the air-surface exchange of HONO in rural forested environments, Geophy. Res. Lett., 33, L02813, doi:10.1029/2005GL024348, 2006.

Heland, J., Kleffmann, J., Kurtenbach, R., and Wiesen, P.: A new instrument to measure gaseous nitrous acid (HONO) in the atmosphere, Environ. Sci. Technol., 35, 3207–3212, 2001.

Honrath, R. E., Lu, Y., Peterson, M. C., Dibb, J. E., Arsenault, M. A., Cullen, N. J., and Steffen, K.: Vertical fluxes of NO$_x$, HONO, and HNO$_3$ above the snowpack at Summit, Greenland, Atmos. Environ., 36, 2629–2640, 2002.

Hu, M., Zhou, F., Shao, K., Zhang, Y., Tang, X., and Slanina, J.: Diurnal variations of aerosol chemical compositions and related gaseous pollutants in Beijing and Guangzhou, J. Environ. Sci. Heal. A, 37, 479–488, 2002.

Huang, G., Zhou, X., Deng, G., Qiao, H., and Civerolo, K.: Measurements of atmospheric nitrous acid and nitric acid, Atmos. Environ., 36, 2225–2235, 2002.

IPCC: Climate Change 2001: The Scientific Basis: Contribution of Working Group I to the Third Assessment Report of the Intergovernmental Panel on Climate Change, Cambridge University Press, Cambridge, UK, 944 pp, 2001.

Israelachvili, J. N. and Pashley, R. M.: Molecular layering of water at surfaces and origin of repulsive hydration forces, Nature, 306, 249–250, 1983.

Kanda, Y. and Taira, M.: Chemiluminescent method for continuous monitoring of nitrous-acid in ambient air, Anal. Chem., 62, 2084–2087, 1990.

Kang, C. M., Kang, B. W., and Lee, H. S.: Source identification and trends in concentrations of gaseous and fine particulate principal species in Seoul, South Korea, J. Air Waste Manag. Assoc., 56, 911–921, 2006.

Karagulian, F. and Rossi, M. J.: Heterogeneous chemistry of the NO$_3$ free radical and N$_2$O$_5$ on decane flame soot at ambient temperature: reaction products and kinetics, J. Phys. Chem. A, 111, 1914–1926, 2007.

Kirchner, U., Scheer, V., and Vogt, R.: FTIR spectroscopic investigation of the mechanism and kinetics of the heterogeneous reactions of NO$_2$ and HNO$_3$ with soot, J. Phys. Chem. A, 104, 8908–8915, 2000.

Kirchner, W., Welter, F., Bongartz, A., Kames, J., Schweighoefer, S., and Schurath, U.: Trace gas exchange at the air/water interface: measurements of mass accommodation coefficients, J. Atmos. Chem., 10, 427–449, 1990.

Kirchstetter, T. W., Harley, R. A., and Littlejohn, D.: Measurement of nitrous acid in motor vehicle exhaust, Environ. Sci. Technol., 30, 2843–2849, 1996.

Kleffmann, J., Becker, K. H., and Wiesen, P.: Heterogeneous NO$_2$ conversion processes on acid surfaces: possible atmospheric implications, Atmos. Environ., 32, 2721–2729, 1998a.

Kleffmann, J., Becker, K. H., and Wiesen, P.: Investigation of the heterogeneous NO$_2$ conversion on perchloric acid surfaces, J. Chem. Soc. Faraday Trans., 94, 3289–3292, 1998b.

Kleffmann, J., Heland, J., Kurtenbach, R., Lorzer, J., and Wiesen, P.: A new instrument (LOPAP) for the detection of nitrous acid (HONO), Environ. Sci. Pollut. Res, 48–54, 2002.

Kleffmann, J., Kurtenbach, R., Lorzer, J., Wiesen, P., Kalthoff, N., Vogel, B. and Vogel, H.: Measured and simulated vertical profiles of nitrous acid. Part I: field measurements, Atmos. Environ.,

37, 2949–2955, 2003.

Kleffmann, J. and Wiesen, P.: Heterogeneous conversion of NO$_2$ and NO on HNO$_3$ treated soot surfaces: atmospheric implications, Atmos. Chem. Phys., 5, 77–83, 2005, http://www.atmos-chem-phys.net/5/77/2005/.

Kleffmann, J.: Daytime sources of nitrous acid (HONO) in the atmospheric boundary layer, Chem. Phys. Chem., 8, 1137–1144, 2007.

Kondo, A., Shrestha, M., Kaga, A., Inoue, Y., and Sapkota, B.: Comparison of field observation with water tank experiment on air pollution concentration in Katmandu valley, Adv. Air Pollut., 11, 493–502, 2002.

Kurtenbach, R., Becker, K. H., Gomes, J. A. G., Kleffmann, J., Lörzer, J. C., Spittler, M., Wiesen, P., Ackermann, R., Geyer, A., and Platt, U.: Investigations of emissions and heterogeneous formation of HONO in a road traffic tunnel, Atmos. Environ., 35, 3385–3394, 2001.

Labban, R., Veranth, J. M., Chow, J. C., Engelbrecht, J. L. P., and Watson, J. G.: Size and geographical variation in PM$_1$, PM$_{2.5}$ and PM$_{10}$: source profiles from soils in the western US, Water Air Soil Pollut., 157, 13–31, 2004.

Lahoutifard, N., Ammann, M., Gutzwiller, L., Ervens, B., and George, Ch.: The impact of multiphase reactions of NO$_2$ with aromatics: a modelling approach, Atmos. Chem. Phys., 2, 215–226, 2002, http://www.atmos-chem-phys.net/2/215/2002/.

Lammel, G. and Perner, D.: The Atmospheric aerosol as a source of nitrous-acid in the polluted atmosphere, J. Aerosol Sci., 19, 1199–1202, 1988.

Lammel, G., and Cape, J. N.: Nitrous acid and nitrite in the atmosphere, Chem. Soc. Rev., 25, 361–369, 1996.

Lammel, G.: Formation of Nitrous Acid: Parameterization and comparison with observations, Max-Planck-Institut für Meteorologie, Hamburg, Germany, 286, 1–36, 1999.

Lee, J. H., and Tang, I. N.: Accommodation coefficient of gaseous NO$_2$ on water surfaces, Atmos. Environ., 22, 1147–1151, 1988.

Li, C. S. and Lin, C. H.: PM$_1$/PM$_{2.5}$/PM$_{10}$ characteristics in the urban atmosphere of Taipei, Aerosol Sci. Technol., 36, 469–473, 2002.

Liao, W., Case, A. T., Mastromarino, J., Tan, D., and Dibb, J. E.: Observations of HONO by laser-induced fluorescence at the South Pole during ANTCI 2003, Geophys. Res. Lett., 33, L09810, doi:09810.01029/02005GL025470, 2006a.

Liao, W., Hecobian, A., Mastromarino, J., and Tan, D.: Development of a photo-fragmentation/laser-induced fluorescence measurement of atmospheric nitrous acid, Atmos. Environ., 40, 17–26, 2006b.

Lin, Y.-C., Cheng, M.-T., Ting, W.-Y., and Yeh, C.-R.: Characteristics of gaseous HNO$_2$, HNO$_3$, NH$_3$ and particulate ammonium nitrate in an urban city of Central Taiwan, Atmos. Environ., 40, 4725–4733, 2006.

Liu, Y. S., Chen, R., Shen, X. X., and Mao, X. L.: Wintertime indoor air levels of PM10, PM2.5 and PM1 at public places and their contributions to TSP, Environ. Int., 30, 189–197, 2004.

Livingston, J. M., and Russell, P. B.: Retrieval of aerosol size distribution moments from multiwavelength particulate extinction measurements, J. Geophys. Res., 94, 8425–8433, 1989.

Longfellow, C. A., Ravishankara, A. R., and Hanson, D. R.: Reactive uptake on hydrocarbon soot: focus on NO$_2$, J. Geophys.

Res., 104, 13833–13840, 1999.

Matsumoto, M., and Okita, T.: Long term measurements of atmospheric gaseous and aerosol species using an annular denuder system in Nara, Japan, Atmos. Environ., 32, 1419–1425, 1998.

Meller, R. and Moortgat, G. K.: Temperature dependence of the absorption cross sections of formaldehyde between 223 and 323 K in the wavelength range 225–375 nm, J. Geophys.Res., 105, 7089–7101, 2000.

Mertes, S., and Wahner, A.: Uptake of nitrogen dioxide and nitrous acid on aqueous surfaces, J. Phys. Chem., 99, 14000–14006, 1995.

Miranda, P. B., Xu, L., Shen, Y. R., and Salmeron, M.: Icelike water monolayer adsorbed on mica at room temperature, Phys. Rev. Lett., 81, 5876–5879, 1998.

Msibi, I. M., Shi, J. P. and Harrison, R. M.: Accommodation coefficient for trace gas uptake using deposition profile measurement in an annular reactor, J. Atmos. Chem., 17, 339–351, 1993.

Nienow, A. M., and Roberts, J. T.: Heterogeneous chemistry of carbon aerosols, Annu. Rev. Phys. Chem., 57, 105–128, 2006.

Notholt, J., and Raes, F.: Test of in situ measurements of atmospheric aerosols and trace gases by long path transmission spectroscopy, J. Aerosol. Sci., 21, S193–S196, 1990.

Notholt, J., Hjorth, J., and Raes, F.: Long path field measurements of aerosol parameters and trace gas concentrations formation of nitrous acid during foggy periods, J. Aerosol. Sci., 22, S411–S414, 1991.

Notholt, J., Hjorth, J., and Raes, F.: Formation of HNO$_2$ on aerosol surfaces during foggy periods in the presence of NO and NO$_2$, Atmos. Environ., 26, 211–217, 1992a.

Notholt, J., Hjorth, J., Raes, F., and Schrems, O.: Simultaneous long path field measurements of HNO$_2$, CH$_2$O and aerosol, Ber. Bunsen. Phys. Chem., 96, 290–293, 1992b.

Opitz, A., Scherge, M., Ahmed, S. I. U., and Schaefer, J. A.: A comparative investigation of thickness measurements of ultrathin water films by scanning probe techniques, J. Appl. Phys., 101, 064310, doi:10.1063/1061.2712155, 2007.

Panday, A.: The diurnal cycle of air pollution in the Kathmandu valley, Nepal, Dept. of Earth, Atmospheric, and Planetary Sciences, Massachusetts Institute of Technology, Cambridge, MA, USA, 100 pp., 2006.

Panday, A.K., and Prinn R. G.: The diurnal cycle of air pollution in the Kathmandu Valley, Nepal: Observations, J. Geophys. Res., 114, D09305, doi:10.1029/2008JD009777, 2009.

Park, S. S., Hong, S. B., Jung, Y. G., and Lee, J. H.: Measurements of PM$_{10}$ aerosol and gas-phase nitrous acid during fall season in a semi-urban atmosphere, Atmos. Environ., 38, 4265–4265, 2004.

Perner, D., and Platt, U.: Detection of nitrous acid in the atmosphere by differential optical absorption, Geophys. Res. Lett., 6, 917–920, 1979.

Pitz, M., Cyrys, J., Karg, E., Wiedensohler, A., Wichmann, H.-E., and Heinrich, J.: Variability of apparent particle density of an urban aerosol, Environ. Sci. Technol., 37, 4336–4342, 2003.

Ponche, J. L., George, C., and Mirabel, P.: Mass transfer at the air/water interface: mass accommodation coefficients of SO$_2$, HNO$_3$, NO$_2$ and NH$_3$, J. Atmos. Chem., 16, 1–21, 1993.

Qin, M., Xie, P. H., Liu, W. Q., Li, A., Dou, K., Fang, W., Liu, H. G., and Zhang, W. J.: Observation of atmospheric nitrous acid with DOAS in Beijing, China, J. Environ. Sci., 18, 69–75, 2006.

Ramanathan, V., Li, F., Ramana, M. V., Praveen, P. S., Kim, D., Corrigan, C. E., Nguyen, H., Stone, E. A., Schauer, J. J., Carmichael, G. R., Adhikary, B., and Yoon, S. C.: Atmospheric brown clouds: hemispherical and regional variations in long-range transport, absorption, and radiative forcing, J. Geophys. Res., 112, D22S21, doi:10.1029/2006JD008124, 2007.

Ramazan, K. A., Wingen, L. M., Miller, Y., Chaban, G. M., Gerber, R. B., Xantheas, S. S., and Finlayson-Pitts, B. J.: New experimental and theoretical approach to the heterogeneous hydrolysis of NO$_2$: key role of molecular nitric acid and its complexes, J. Phys. Chem. A, 110, 6886–6897, 2006.

Regmi, R. P., Kitada, T., and Kurata, G.: Numerical simulation of late wintertime local flows in Kathmandu valley, Nepal: Implication for air pollution transport, J. Appl. Meteorol., 42, 389–403, 2003.

Reisinger, A. R.: Observations of HNO$_2$ in the polluted winter atmosphere: possible heterogeneous production on aerosols, Atmos. Environ., 34, 3865–3874, 2000.

Rohrer, F., Bohn, B., Brauers, T., Brüning, D., Johnen, F.-J., Wahner, A., and Kleffmann, J.: Characterisation of the photolytic HONO-source in the atmosphere simulation chamber SAPHIR, Atmos. Chem. Phys., 5, 2189–2201, 2005, http://www.atmos-chem-phys.net/5/2189/2005/.

Rubio, M.A., Lissi, E., and Villena, G.: Nitrite in rain and dew in Santiago city, Chile. Its possible impact on the early morning start of the photochemical smog, Atmos. Environ., 36, 293–297, 2002.

Saliba, N. A., Mochida, M. and Finlayson-Pitts B. J.: Laboratory studies of sources of HONO in polluted urban atmospheres, Geophys. Res. Lett., 27, 3229–3232, 2000.

Saliba, N. A., Yang, H., and Finlayson-Pitts B. J.: Reaction of gaseous nitric oxide with nitric acid on silica surfaces in the presence of water at room temperature, J. Phys. Chem. A, 105, 10339–10346, 2001.

Sapkota, B. and Dhaubhadel, R.: Atmospheric turbidity over Kathmandu valley, Atmos. Environ., 36, 1249–1257, 2002.

Schuttlefield, J. D., Cox, D., and Grassian, V. H.: An investigation of water uptake on clays minerals using ATR-FTIR spectroscopy coupled with quartz crystal microbalance measurements, J. Geophys. Res., 112, D21303, doi:10.1029/2007JD008973, 2007.

Seinfeld, J. H., and Pandis, S. N.: Atmospheric chemistry and physics: from air pollution to climate change, Wiley & Sons, New York, USA, 250–253, 1998.

Seisel, S., Lian, Y., Keil, T., Trukhin, M. E., and Zellner, R.: Kinetics of the interaction of water vapour with mineral dust and soot surfaces at T=298 K, Phys. Chem. Chem. Phys., 6, 1926–1932, 2004.

Seisel, S., Pashkova, A., Lian, Y., and Zellner, R.: Water uptake on mineral dust and soot: A fundamental view of the hydrophilicity of atmospheric particles?, Faraday Discuss., 130, 437–451, 2005.

Sharma, C. K.: Urban air quality of Kathmandu valley "Kingdom of Nepal", Atmos. Environ., 31, 2877–2883, 1997.

Sharma, T., Rainey, R. C., Neumann, C. M., Shrestha, I. L., Shahi, K. B., Shakya, A., and Khatri, S.: Roadside particulate levels at 30 locations in the Kathmandu Valley, Nepal, Int. J. Environ. Pollut., 17, 293–305, 2002.

Shon, Z.-H., Lee, G., Song, S.-K., Lee, M., Han, J., and Lee, D.: Characteristics of reactive nitrogen compounds and other relevant trace gases in the atmosphere at urban and rural areas of

Korea during May–June, 2004, J. Atmos. Chem., 58, 203–218, 2007.

Spindler, G., Müller, K., Brüggemann, E., Gnauk, T., and Herrmann, H.: Long-term size-segregated characterization of PM$_{10}$, PM$_{2.5}$, and PM$_1$ at the IfT research station Melpitz downwind of Leipzig (Germany) using high and low-volume filter samplers, Atmos. Environ., 38, 5333–5347, 2004.

Stemmler, K., Ammann, M., Donders, C., Kleffmann, J., and George, C.: Photosensitized reduction of nitrogen dioxide on humic acid as a source of nitrous acid, Nature, 440, 195–198, 2006.

Stemmler, K., Ndour, M., Elshorbany, Y., Kleffmann, J., D'Anna, B., George, C., Bohn, B., and Ammann, M.: Light induced conversion of nitrogen dioxide into nitrous acid on submicron humic acid aerosol, Atmos. Chem. Phys., 7, 4237–4248, 2007, http://www.atmos-chem-phys.net/7/4237/2007/.

Stockwell, W. R., and Calvert, J. G.: The Mechanism of NO$_3$ and HONO formation in the nighttime chemistry of the urban atmosphere, J. Geophys. Res., 88, 6673–6682, 1983.

Stutz, J., and Platt, U.: Numerical analysis and estimation of the statistical error of differential optical absorption spectroscopy measurements with least-squares methods, Appl. Optics, 30, 6041–6053, 1996.

Stutz, J., Kim, E. S., Platt, U., Bruno, P., Perrino, C., and Febo, A.: UV-visible absorption cross sections of nitrous acid, J. Geophys. Res. 105, 14585–14592, 2000.

Stutz, J., Alicke, B., Ackermann, R., Geyer, A., Wang, S., White, A. B., Williams, E. J., Spicer, C. W., and Fast, J. D.: Relative humidity dependence of HONO chemistry in urban areas, J. Geophys. Res., 109, D03307, doi:10.1029/2003JD004135, 2004.

Su, H., Cheng, Y., Shao, M., Gao, D., Yu, Z., Zeng, L., Slanina, J., Zhang, Y., and Wiedensohler, A.: Nitrous acid (HONO) and its daytime sources at a rural site during the 2004 PRIDE-PRD experiment in China, J. Geophys. Res., 113, D14312, doi:10.1029/2007JD009060, 2008a.

Su, H., Cheng, Y., Cheng, P., Zhang, Y., Dong, S., Zeng, L., Wang, X., Slanina, J., Shao, M., and Wiedensohler, A.: Observation of nighttime nitrous acid (HONO) formation at a non-urban site during PRIDE-PRD2004 in China, Atmos. Environ., 42, 6219–6232, 2008b.

Sumner, A. L., Menke, E. J., Dubowski, Y., Newberg, J. T., Penner, R. M., Hemminger, J. C., Wingen, L. M., Brauers, T., and Finlayson-Pitts, B. J.: The Nature of water on surfaces of laboratory systems and implications for heterogeneous chemistry in the troposphere, Phys. Chem. Chem. Phys., 6, 604–613, 2004.

Svensson, R., Ljungström, E., and Lindqvist, O: Kinetics of the reaction between nitrogen dioxide and water vapour, Atmos. Environ., 21, 1529–1539, 1987.

Syomin, D. A., and Finlayson-Pitts, B. J.: HONO decomposition on borosilicate glass surfaces: implications for environmental chamber studies and field experiments, Phys. Chem. Chem. Phys., 5, 5236–5242, 2003.

Takenaka, N., Terada, H., Oro, Y., Hiroi, M., Yoshikawa, H., Okitsu, K., and Bandow, H.: A new method for the measurement of trace amounts of HONO in the atmosphere using an air-dragged aqua-membrane-type denuder and fluorescence detection, Analyst, 129, 1130–1136, 2004.

Trebs, I., Meixner, F. X., Slanina, J., Otjes, R., Jongejan, P., and Andreae, M. O.: Real-time measurements of ammonia, acidic trace gases and water-soluble inorganic aerosol species at a rural site

in the Amazon Basin, Atmos. Chem. Phys., 4, 967–987, 2004, http://www.atmos-chem-phys.net/4/967/2004/.

Trick, S.: Formation of nitrous acid on urban surfaces: a physical chemical perspective, Fakultät für Naturwissenschaften und Mathematik, University of Heidelberg, Heidelberg, Germany, 290 pp, 2004.

Vallius, M. J., Ruuskanen, J., Mirme, A., and Pekkanen, J.: Concentrations and estimated soot content of PM$_1$, PM$_{2.5}$, and PM$_{10}$ in a subarctic urban atmosphere, Environ. Sci. Technol., 34, 1919–1925, 2000.

Večeřa, Z. and Dasgupta, P. K.: Measurement of ambient nitrous acid and a reliable calibration source for gaseous nitrous-acid, Environ. Sci. Technol., 25, 255–260, 1991.

Vandaele, A.C., Hermans, C., Fally, S., Carleer, M., Colin, R., Mérienne, M.-F., and Jenouvrier, A.: High-resolution Fourier transform measurement of the NO$_2$ visible and near-infrared absorption cross-section: Temperature and pressure effects, J. Geophys. Res. 107, 4348, doi:10.1029/2001JD000971, 2002.

Vogel, B., Vogel, H., Kleffmann, J., and Kurtenbach, R.: Measured and simulated vertical profiles of nitrous acid – Part II. model simulations and indications for a photolytic source, Atmos. Environ., 37, 2957–2966, 2003.

Wang, S., Ackermann, R., Spicer, C. W., Fast, J. D., Schmeling, M., and Stutz, J.: Atmospheric observations of enhanced NO$_2$-HONO conversion on mineral dust particles, Geophys. Res. Lett., 30, 1595, doi:10.1029/2003GL017014, 2003.

World Bank: Urban air quality management strategy in Asia (UR-BAIR), Kathmandu valley., Technical paper 378, 157 pp, 1997.

Wormhoudt, J., Herndon, S. C., Yelvington, P. E., Miake-Lye, R. C., and Wey, C.: Nitrogen oxide (NO/NO$_2$/HONO) emissions measurements in aircraft exhausts, J. Propul. Power, 23, 906–911, 2007.

Yu, Y., Geyer, A., Xie, P., Galle, B., Chen, L., and Platt, U.: Observations of carbon disulfide by differential optical absorption spectroscopy in Shanghai, Geophys. Res. Lett., 31, L11107, doi:11110.11029/GL019543, 2004.

Yu, Y., Panday, A., Hodson, E., Galle, B., and Prinn R.: Monocyclic aromatic hydrocarbons in Kathmandu during the winter season, Water Air Soil Pollut., 191, 71–81, 2008a.

Yu, Y., Ezell, M. J., Zelenyuk, A., Imre, D., Alexander, M. L., Ortega, J., D'Anna, B., Harmon, C. W., Johnson, S. N., and Finlayson-Pitts, B. J.: Photooxidation of α-pinene at high relative humidity in the presence of increasing concentrations of NO$_x$, Atmos. Environ., 42, 5044–5060, 2008b.

Zhang, J., Wang, T., Chameides, W. L., Cardelino, C., Kwok, J., Blake, D. R., Ding, A., and So, K. L.: Ozone production and hydrocarbon reactivity in Hong Kong, Southern China, Atmos. Chem. Phys., 7, 557–573, 2007, http://www.atmos-chem-phys.net/7/557/2007/.

Zhou, X., Civerolo, K., Dai, H., Huang, G., Schwab, J., and Demerjian, K.: Summertime nitrous acid chemistry in the atmospheric boundary layer at a rural site in New York State, J. Geophys. Res., 107, 4590, doi:10.1029/2001JD001539, 2002.

Zhou, X., Beine, H. J., Honrath, R. E., Fuentes, J. D., Simpson, W., Shepson, P. B., and Bottenheim, J. W.: Snowpack photochemical production of HONO: a major source of OH in the Arctic boundary layer in springtime, Geophys. Res. Lett., 28, 4087–4090, 2001.

Zhou, X., Huang, G., Civerolo, K., Roychowdhury, U., and Demerjian, K. L.: Summertime observations of HONO, HCHO, and O$_3$ at the summit of Whiteface Mountain, New York, J. Geophys. Res., 112, D08311, doi:10.1029/2006JD007256, 2007.